Molecular Crystals and Liquid Crystals

ISSN: 1542-1406 (Print) 1563-5287 (Online) Journal homepage: http://www.tandfonline.com/loi/gmcl20

Interaction of Nano-Clay Platelets with a Phospholipid in Presence of a Fluorescence Probe

Mitu Saha, S. A. Hussain & D. Bhattacharjee

To cite this article: Mitu Saha, S. A. Hussain & D. Bhattacharjee (2015) Interaction of Nano-Clay Platelets with a Phospholipid in Presence of a Fluorescence Probe, Molecular Crystals and Liquid Crystals, 608:1, 198-210, DOI: 10.1080/15421406.2014.950465

To link to this article: http://dx.doi.org/10.1080/15421406.2014.950465

Mol. Cryst. Liq. Cryst., Vol. 608: pp. 198–210, 2015

ISSN: 1542-1406 print/1563-5287 online
DOI: 10.1080/15421406.2014.950465

Taylor & Francis
Taylor & Francis Group

Interaction of Nano-Clay Platelets with a Phospholipid in Presence of a Fluorescence Probe

MITU SAHA, S. A. HUSSAIN, AND D. BHATTACHARJEE*

Department of Physics, Tripura University, Suryamaninagar, Tripura, India

This paper reports the interaction of nano-clay platelets with a phospholipid in presence of a fluorescence probe. The surface pressure vs. time characteristic studies were done to monitor the progress of reaction. In-situ fluorescence imaging microscope (FIM) was employed to visualize the domain structure formed at the air-water interface with the progress of reaction. At the end of the reaction, clay induced hybrid monolayer at the air-water interface was transferred onto solid substrate to form Langmuir Blodgett (LB) film. Fluorescence spectroscopic studies revealed the close proximity of RhB molecules resulting in the formation of dimeric species.

Keywords DPPC; FIM; laponite; pressure-area isotherm; reaction kinetics; RhB

1. Introduction

Insoluble monolayer formed by spreading of amphiphilic molecules at the air-water interface are known as Langmuir monolayer. Langmuir monolayer has been widely investigated by the analysis of the surface pressure—area per molecule (π-A) isotherms which provides a well-defined, two-dimensional medium where molecular orientation, packing density, phase behavior, and surface tension can be controlled by changing various parameters. Study of this monolayer is important for molecular interactions especially for biomembranes [1–3]. Investigations of molecular interactions have been done by studying the effects of nano-particulate materials on the bio-physical behavior of Langmuir monolayer [4–7]. Recent interest lies on the studies of the nano-particle interactions with the Langmuir monolayer of biomolecules and provide important applications in various fields such as occupational health [8], food [9], cosmetics [10], and pharmaceuticals [11]. The interactions of nano-particulate materials can change the biophysical behavior of Langmuir monolayer of the biomolecules. The size and large surface area-to-volume ratio of nano-particles modify the phase behavior and the structure of the monolayer. Depending on the various types of the nano-particles such types of interactions can be used as model systems in several fields of biological systems, biomembranes [12], respiratory physiology [13, 14]. The study of the effect of nano-particles on the biological system is an important topic in environmental study and also in nano-materials [15–18].

Recently immense interests have been given to the study of naturally occurred nano-clay materials which is technologically as well as biologically important [19–21].

*Address correspondence to D. Bhattacharjee, Department of Physics, Tripura University, Suryamaninagar -799022, Tripura, India. E-mail: debu@tripurauniv.in

Color versions of one or more of the figures in the article can be found online at www.tandfonline.com/gmcl.

In the field of the bionanoscience, nano-clay particles give an opportunity to the researchers to know about the interaction of nano-clay particles with the biomolecules. Works are going on where the researchers focused on the preparation of hybrid protein-clay films used as a biological model system [22]. In a recent work, Guocheng et al. studied the mechanism of adsorption of acridine orange (AO), a cationic dye, on low charge montmorillonite clay which helps to remove the AO from the domestic wastewater [23]. Such types of works have technological importance in the field of bionanoscience which helps to protect the environment from various types of pollutions.

Here, we have studied the effect of nano-clay particles on the lung surfactant phospholipid 1, 2-dipalmitoyl-sn-glycero-3-phosphocholine (DPPC) monolayer. DPPC is a zwitterionic phospholipid capable of forming stable Langmuir monolayer at the air-water interface. Langmuir monolayer resembles an ideal model for the studies of phospholipids, proteins, pulmonary surfactants, organic, inorganic, and other amphiphilic molecules [24–29]. DPPC is the main phospholipids component of natural pulmonary surfactant. The Langmuir monolayer of DPPC molecules at the air-water interface comprises a biological model system for phospholipid studies. The properties and phase behavior of this monolayer have been extensively investigated by a variety of techniques. The phase transitions of lipid monolayer are very important in respect to different physiological functions [30, 31].

Sabina et al. [32] studied the effect of gold nano-particles on the phase behavior of DPPC monolayer at the air-water interface. The presence of gold nano-particles significantly affected the domain formation of DPPC at the air-water interface which was observed by BAM studies. Eduardo Guzman et al. [33] analyzed the impact of silica nano-particles on the thermodynamic characteristics and structural properties of DPPC-Palmitic acid (PA) Langmuir monolayer relevant in the field of lung surfactant. The significant effect of silica nano-particles was observed on the domain formation of DPPC and PA monolayer at the air-water interface using BAM study. The changes in the DPPC and PA monolayers give a rough model of the pulmonary surfactant which also provides information applicable to realistic systems. In another work [34] effect of silica nano-particles on the phase behavior of DOPC and DOPC-DPPC monolayer have been studied. It has been observed that silica nano-particles have important effects on the physicochemical properties of lipid monolayer especially concerning their response to periodic area deformations. Farnoud et al. [35] studied the effect of negatively charged carboxyl modified polystyrene (CML) submicron particles on the DPPC monolayer at the air-water interface. The microstructure of DPPC monolayer was studied by using Fluorescence Imaging Microscope (FIM). The presence of CML particles resulting in the formation of smaller, but more numerous domains at the air water interface. In the FIM study, Texas-Red DHPE was used as a fluorescent probe.

In our present investigation on the interactions of nano-clay particles with DPPC monolayer, FIM images showed large concentrations of domain structures resulting due to the introduction of nano-clay particles. Rhodamine B (RhB) was used as a fluorescent probe. Rhodamine B (RhB) is a xanthene molecular dye with outstanding spectral luminescence properties and has vast applications in the study of various objects including biological systems, sensors and markers based on thin films [36], laser technology [37], in supramolecular chemistry [38], and in studies of nano-objects [39]. In case of biological device applications, RhB is required to be embedded in a solid matrix or to incorporate into ordered ultrathin films.

Spectroscopic investigations revealed the aggregation of RhB molecules on the clay particles. As a result dimeric sites of RhB molecules became predominant.

2. Experimental Section

1,2-dipalmitoyl-sn-glycero-3-phosphocholine (DPPC) and Rhodamine B (RhB) (purity >99%), were purchased from Sigma Chemical Company and used without further purification. Purity of the samples were checked by UV-Vis absorption and fluorescence spectroscopic techniques. The clay mineral used in the present work was laponite, obtained from Laponite Inorganics, UK and was used as received. The size of the clay platelet was less than 0.05 μm and its cation exchange capacity (CEC) was 0.74 meq/g. The clay minerals were stored as freeze dried powders. Chloroform (SRL, India) used as a solvent, was of spectroscopic grade and its purity was checked by fluorescence spectroscopy.

Surface pressure vs. area per molecule (π-A) isotherm, surface pressure vs. time (π-t) characteristic study, and LB film preparation were done by using LB film deposition instrument (APEX-2000C, India). FIM studies were done by using in situ FIM (Motic AE 31) attached with the LB instrument. Ultra pure Milli-Q (resistivity 18.2 MΩ cm) water was used as the subphase and for the preparation of the aqueous solution of RhB. The temperature was maintained at 24°C throughout the experiment.

To record the Surface pressure vs. area per molecule (π-A) isotherms of DPPC on pure water subphase and clay dispersed subphase containing aqueous solution of RhB, dilute chloroform solution of DPPC was spread at either air-water interface or air-clay dispersion interface. After allowing sufficient time to evaporate the solvent, the barrier was compressed slowly to obtain the isotherm characteristics. To study the DPPC isotherm on the RhB mixed clay dispersed subphase, 50 μl of DPPC (Concentration 1 mM) was spread onto the RhB mixed (100 μl, Concentration 1 mM) aqueous clay dispersion subphase. Clay concentration was 2 ppm. After spreading chloroform solution of DPPC on the subphase, sufficient time was allowed for completing the reaction between DPPC, RhB and clay platelets. The barrier was compressed slowly to obtain the isotherm characteristics.

Surface pressure vs. time (π-t) characteristic curve was recorded to monitor the progress of reaction. To obtain this characteristic, first of all 50 μl chloroform solution of DPPC was spread on either pure water or clay dispersed aqueous subphase on the LB trough. After allowing 15 minutes to evaporate the solvent, the barrier was compressed slowly to obtain the nominal surface pressure of 0.1 mN/m and then the barrier was kept fixed. After waiting for few minutes to stablize the monolayer, 100 μl of aqueous solution of RhB of concentration 1 mM was injected from the back side of the barrier so as not to disturb the preformed DPPC monolayer. Being water soluble, RhB molecules started crossing the barrier through the subphase and moved up and interacted with the anionic clay platelets as well as zwitterionic DPPC molecules in the preformed monolayer. As a result, RhB-DPPC-clay hybrid monolayer was formed at the air-water interface. With the passage of time, the number of RhB-DPPC-clay hybrid molecules at the air-water interface increased. The area per molecule of this hybrid molecule is greater than the area per molecule of pure DPPC. But as the barrier was kept fixed at a particular position, hence the tendency to increase the area per molecule was consequently manifested by the increase in surface pressure. The increase in surface pressure with time was recorded to have the surface pressure vs. time (π-t) curve. Surface pressure was recorded using Wilhelmy plate arrangement as described elsewhere [40, 41].

The surface morphology of the Langmuir monolayer at the air-water interface was changed with the progress of reaction. The direct visual images of the surface morphology at the air-water interface were obtained by in-situ FIM attached with the LB instrument.

After completion of the reaction, the hybrid films were transferred onto the fluorescence grade quartz substrates to form mono- and multilayer LB films.

UV-Vis absorption and fluorescence spectra were recorded by UV-Vis absorption spectrophotometer (Lambda 25, Perkin Elmer) and fluorescence spectrophotometer (LS 55, Perkin Elmer).

3. Results and Discussions

3.1. Surface Pressure vs. Area per Molecule (π-A) Isotherm

Figure 1(a) shows the surface pressure vs. area per molecule (π-A) isotherms of DPPC on pure water subphase (graph I) and on clay-dispersed subphase (graph II). DPPC isotherm on pure water subphase exhibits a plateau [42, 43] with an initial lift-off area of 1.15 nm^2. DPPC isotherm on clay dispersed aqueous subphase also shows a plateau with an initial lift-off area of 1.23 nm^2, which is larger than pure DPPC isotherm at the air-water interface. This indicates an interaction with the anionic clay platelets with the zwitterionic DPPC molecules on the surface. Due to adsorption of DPPC molecules on the clay platelets molecular organization changes resulting in the increase of initial lift off area.

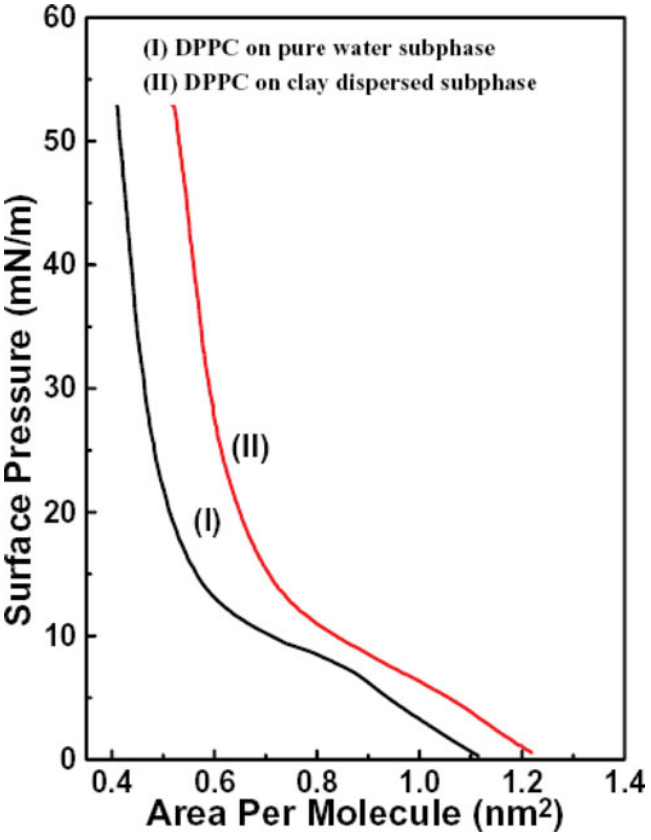

Figure 1. (a) Surface pressure vs. area per molecule (π-A) isotherms of DPPC on (I) pure water subphase and (II) 2 ppm clay dispersed subphase.

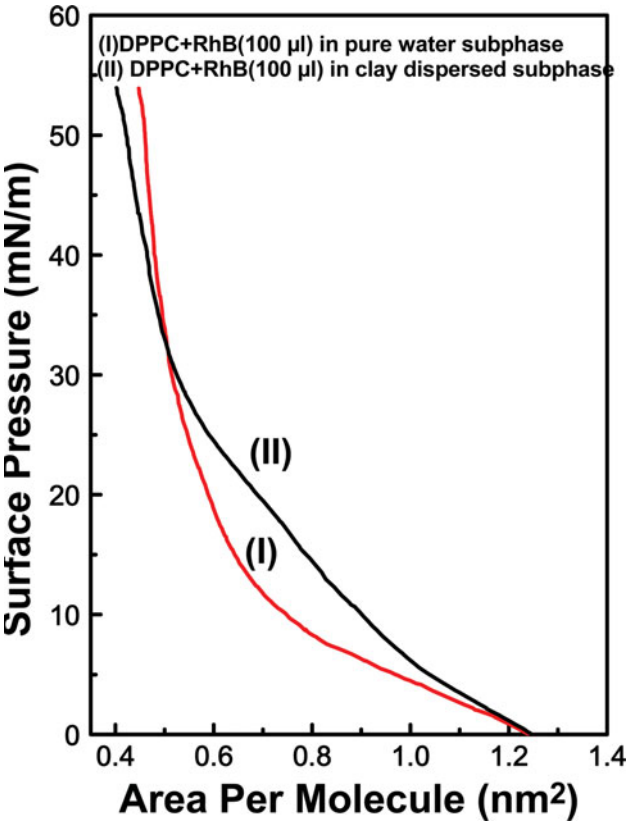

Figure 1. **(b)** Surface pressure vs. area per molecule (π-A) isotherms of DPPC on (I) 100 μl RhB mixed aqueous subphase and (II) 100 μl RhB in 2 ppm clay dispersed subphase.

Figure 1(b) shows the surface pressure vs. area per molecule (π-A) isotherms of DPPC monolayer in RhB mixed subphase (graph I) and in RhB-clay dispersed subphase (graph II). Amount of RhB was 100 μl, 1 mM concentration in every cases and clay concentration was 2 ppm. In both the cases isotherms started rising with nearly equal initial lift off area 1.23 nm^2, which was same with the initial lift off area of DPPC isotherm in the clay dispersed aqueous subphase. This may be due to the fact that at the initial stage of the liquid expanded (LE) phase, clay platelets do not have any influence on the molecular organization in presence of RhB molecules. That's why the lift-off areas of the isotherms in RhB-clay dispersed subphase are nearly same as that of the lift-off area of DPPC isotherm in clay subphase. But in the liquid condensed (LC) and in the solid phase of the isotherm (graph II) organization of DPPC molecules at the air-water interface was changed due to the influence of clay platelets. As a result area per molecule of the DPPC isotherms in LC and solid phase are different for different isotherms. This indicates definite interaction of DPPC with RhB and clay platelets at the air-water interface.

3.2. Surface Pressure vs. Time (π-t) Curve

Figure 2 shows the surface Pressure (π) vs. time (t) characteristic curves of DPPC monolayer on pure water subphase (graph I) and 2 ppm clay dispersed water subphase (graph II).

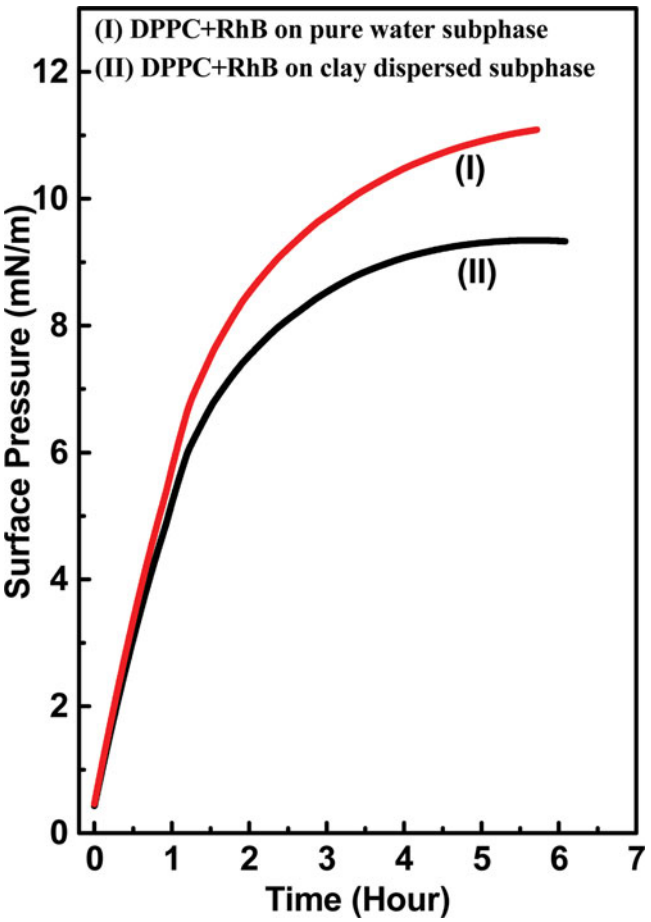

Figure 2. Surface pressure vs. time (π-t) curve of DPPC monolayer when RhB (100 μl) is injected in (I) pure water subphase and (II) 2 ppm clay dispersed subphase.

100 μl solutions (1 mM) of RhB were injected from the back side of the barrier so as not to disturb the preformed DPPC monolayer at the air-water interface. Being water soluble, RhB molecules crossed the barrier through the subphase and moved up and interacted with the anionic clay platelets as well as zwitterionic DPPC molecules in the preformed monolayer. A hybrid Langmuir monolayer started to form. The area per molecule of this hybrid monolayer was greater than the area per molecule of preformed DPPC monolayer. As a result surface pressure tried to increase, but since the barrier was kept fixed at a particular position therefore this tendency to increase the area per molecule was manifested as the increase in surface pressure with the progress of time. At the end, a plateau was observed indicating the end of adsorption process and completion of the formation of hybrid monolayer. In absence of clay platelets, the plateau region was achieved (graph I) at a higher surface pressure than that in presence of clay platelets (graph II). It indicates that in presence of clay platelets in the aqueous subphase, RhB molecules interacted both with DPPC molecules and clay platelets, and few of this RhB adsorbed clay platelets did not come to the surface to interact with the DPPC molecules in the monolayer. They did

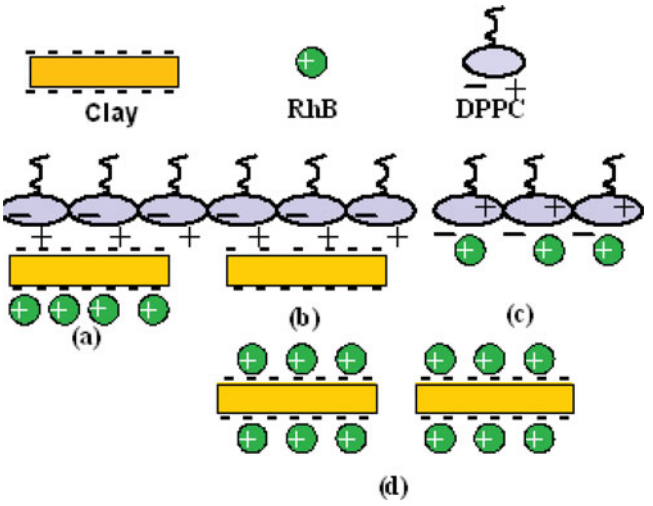

Figure 3. A schematic representation of the adsorption of DPPC and RhB on the clay platelets.

not give any contribution to the hybrid monolayer. As a result, in the second case (graph II) adsorption process was completed at a lower surface pressure.

3.3. Schematic Representation

Figure 3 shows a schematic representation of the adsorption of DPPC and RhB on the clay surface. Four types of adsorption schemes may be possible. In scheme (a), DPPC molecules in the preformed monolayer and RhB molecules in the subphase may be simultaneously adsorbed onto the clay platelets to form a hybrid structure. In scheme (b), only DPPC molecules in the preformed monolayer may be adsorbed on the clay platelets and thus only DPPC-clay hybrid structure is formed. In scheme (c), RhB molecules in the subphase may be adsorbed to the DPPC molecules in the preformed monolayer. Finally in scheme (d), RhB molecules in the subphase are adsorbed onto the clay platelets within the subphase. Thus RhB-clay hybrid structure may be formed. In the clay, dispersed subphase a large amount of RhB molecules may interact with the clay platelets in the dispersion and few clay platelets are left to interact with the DPPC molecules in the preformed monolayer.

3.4. In-situ FIM Studies of Hybrid Monolayer during Isotherm Measurement

In-situ FIM technique has been employed to study the hybrid monolayer film at the air-water interface. Figure 4 shows the FIM images of DPPC-RhB-Clay hybrid monolayer at different surface pressures as indicated in the isotherm curve. In this case, 100 μl, 1 mM concentration of RhB solution was mixed with 2 ppm clay dispersed aqueous subphase. After spreading the dilute chloroform solution of DPPC (50 μl) on the subphase and after sufficient time was allowed to complete the reaction, DPPC-RhB-Clay hybrid monolayer was formed at the air-water interface.

The (π-A) isotherm characteristics of this hybrid monolayer was discussed before. FIM image of RhB-clay mixed subphase in absence of DPPC was found to have uniform bright crimson red background (Fig. 4(a)) due to the presence of highly fluorescent RhB molecules in the subphase. After spreading the DPPC molecules at the air-water interface and at the

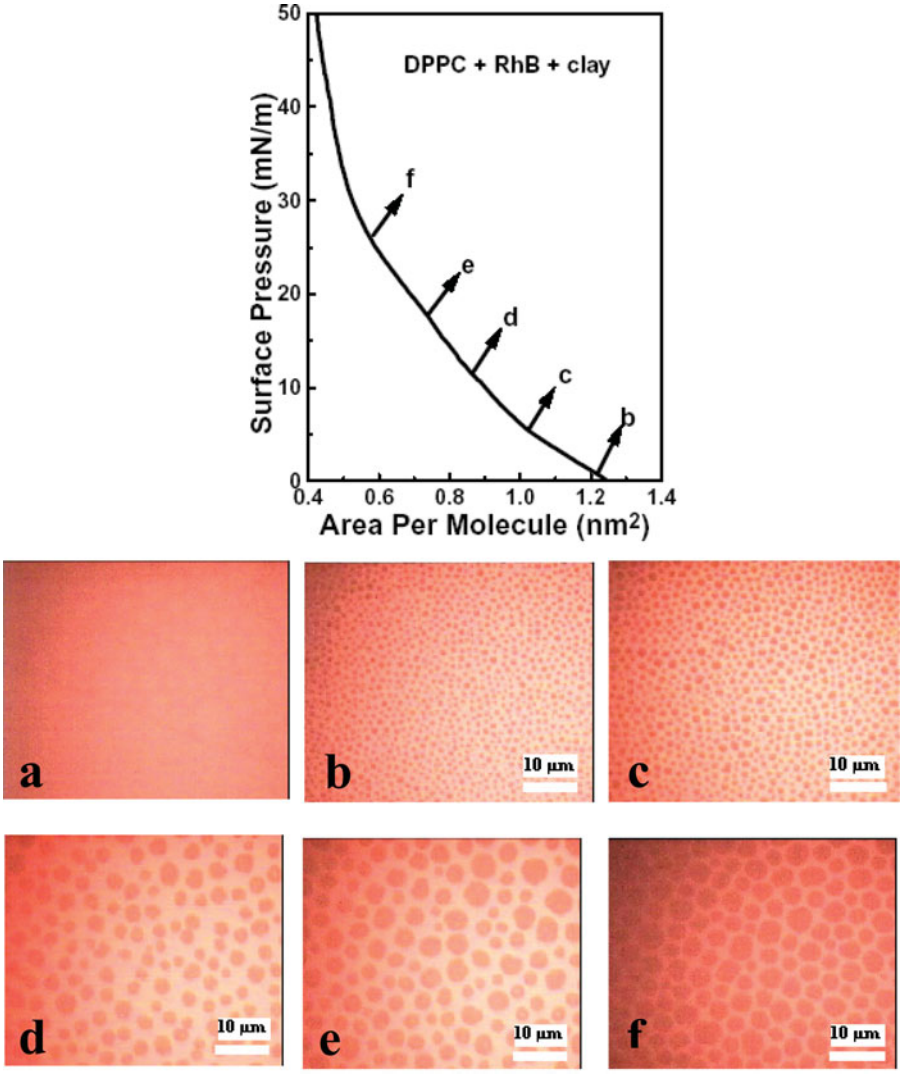

Figure 4. In-situ fluorescence microscope images of Langmuir monolayer of DPPC in RhB (100 μl) mixed clay dispersed subphase during compression at different surface pressures (b) 0.76 mN/m, (c) 5.54 mN/m, (d) 11.4 mN/m, (e) 17.7 mN/m, and (f) 26 mN/m and figure (a) represents the surface image before spreading the DPPC solution. The scale bar in the lower right represents 10 μm. Corresponding (π-A) isotherm and the positions where images were taken are also shown in the figure.

initial stage of the pressure area isotherm (surface pressure $\sim$1 mN/m) nucleation and growth of tiny domains were observed in the monolayer (Fig. 4(b)). With further increase of surface pressure, the density as well as dimension of the tiny domains increased (Fig. 4(c)). At higher surface pressure, the tiny domains coalesced to form larger domains. The density of the larger domain also increased and they overlapped on each other to form almost a black surface (Figs. 4(d)–(f)). The domains were formed due to aggregation of large number of DPPC-RhB-Clay platelets at the air-water interface. The presence of large

number of domains at the air-water interface may be due to clay platelets. Clay platelets provided a platform for concentrating the DPPC and RhB molecules due to which the domains produced were comparatively large in number. Independent of the ratio of the DPPC and RhB in the clay subphase, domains were circular in shape and grew in size upon further compression of the monolayer. Clay platelets also gave a regular arrangement of the domains at the air-water interface. The domains became less prominent at higher surface pressure. It indicates that the domains have been merged and formed uniform monolayer.

3.5. In-situ FIM Studies of Hybrid Monolayer during (π-t) Characteristic Study

Surface pressure vs. time (π-t) characteristic curve demonstrated the progress of reaction to form hybrid films of DPPC-RhB-Clay at the air-water interface and has been discussed in the previous section. During the progress of adsorption process, the nature of domain structures formed at the air–water interface can be visualized by employing in-situ FIM studies at different time intervals. Before injecting the RhB molecules, the surface was totally black indicating the absence of highly fluorescent RhB molecules in the subphase (Fig. 5(a)). When dilute solution of RhB was injected in the back side of the barrier, being water soluble RhB molecules crossed the barrier through the subphase and got adsorbed onto the clay platelets in the subphase as well as to the DPPC molecules in the preformed monolayer. Consequently, DPPC-RhB-Clay hybrid structure was formed. The area per molecule of this hybrid monolayer was greater than pure DPPC monolayer, as a result surface pressure increased. Due to predominance of cohesive force the hybrid molecules formed clusters. As a result small domains were started to form at the air–water interface due to aggregation. Even at a smaller surface pressure of 2.5 mN/m large number of crimson red small domains became visible (Fig. 5(b)). At higher surface pressure of about 5 mN/m smaller domains started to coalesce to form larger crimson red domains (Fig. 5(c)) against a black background. With further increase of surface pressure domains became larger, shaped almost like elliptical (Figs. 5(d)–(f)), the background became black. The highly fluorescent crimson red domains indicated the presence of RhB molecules. The black background was the rest of the surface where RhB molecules were absent. After attaining the stable surface pressure large crimson red domains of the hybrid molecules became visible against the black background (Fig. 5(f)). It indicates that at the end of the adsorption process all the RhB molecules were adsorbed and no RhB molecules were left in the subphase. As a result, the surface became black. Also the hybrid monolayer covered a large portion of the surface area.

3.6. UV-Vis Absorption and Steady State Fluorescence Spectroscopic Studies

UV-Vis absorption and steady state fluorescence spectra of aqueous solution of RhB (10^{-6} M), RhB microcrystal, 10 bilayer of hybrid LB film in absence, and in presence of clay platelets are shown in Figs. 6(A)–(B). LB film deposition was done after stable surface pressure was achieved during adsorption process (π-t curve). DPPC being a non-fluorescent material has no contribution to the absorption and fluorescence spectra in the visible range. Being highly fluorescent only RhB molecules may contribute to the absorption and fluorescence spectra in the visible range. UV-Vis absorption spectrum of pure RhB in dilute aqueous solution (10^{-6} M) possesses intense band with peak at 553 nm along with a shoulder at about 515 nm. The 553 nm band is due to the 0–0 absorption and trace of monomer, where as the 515 nm weak shoulder is assigned to be due to the 0-1 vibronic transition of monomer [44]. These two bands in microcrystal absorption spectrum are red

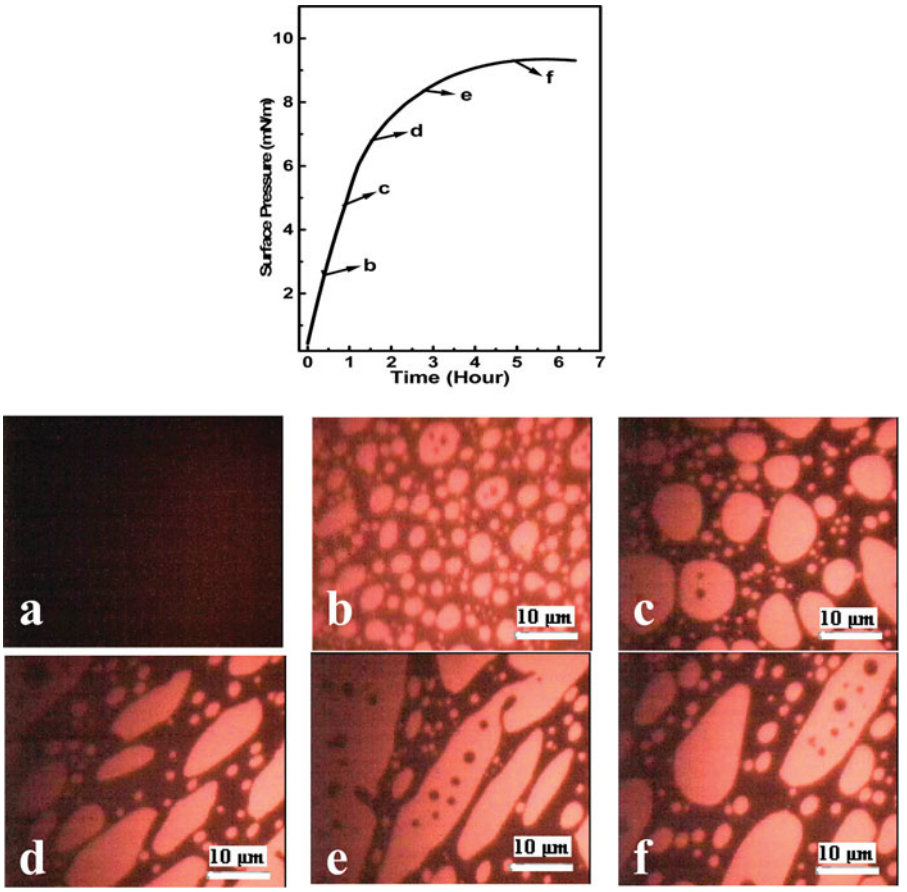

Figure 5. In-situ Fluorescence Microscope Images taken during adsorption process at different surface pressures viz. (b) 2.6 mN/m, (c) 4.7 mN/m, (d) 6.8 mN/m, (e) 8.38 mN/m, and (f) 9.3 mN/m and figure (a) represents the surface image before injecting the RhB solution. The scale bar in the lower right represents 10 μm. Corresponding (π-t) curve and the positions where images were taken are also shown in the figure.

shifted to 572 nm and 530 nm respectively. LB film absorption spectra both in presence and absence of clay also possess almost similar spectral profile to that of microcrystal.

The red shifting of absorption bands in the LB film and microcrystal may be due to the effect of microenvironment when the molecules were transferred from solution to the restricted geometry of solid surface. This in turn affected the electronic energy levels resulting in the change of intensity and band shift in the spectra.

The fluorescence spectrum of RhB aqueous solution shows intense band with peak at 580 nm. In microcrystal fluorescence spectrum, an intense longer wavelength band at about 642 nm was developed and the intensity of 571 nm band was reduced to a larger extent.

DPPC-RhB hybrid LB film in absence of clay also gives same spectral profile to that of microcrystal RhB spectrum. Bur there is a difference in the intensity ratio of the two bands and longer wavelength band positions are slightly different. This longer wavelength band has been assigned as due to the presence of dimeric species [45]. The most interesting observation is that when the same hybrid LB film of DPPC-RhB was fabricated in presence

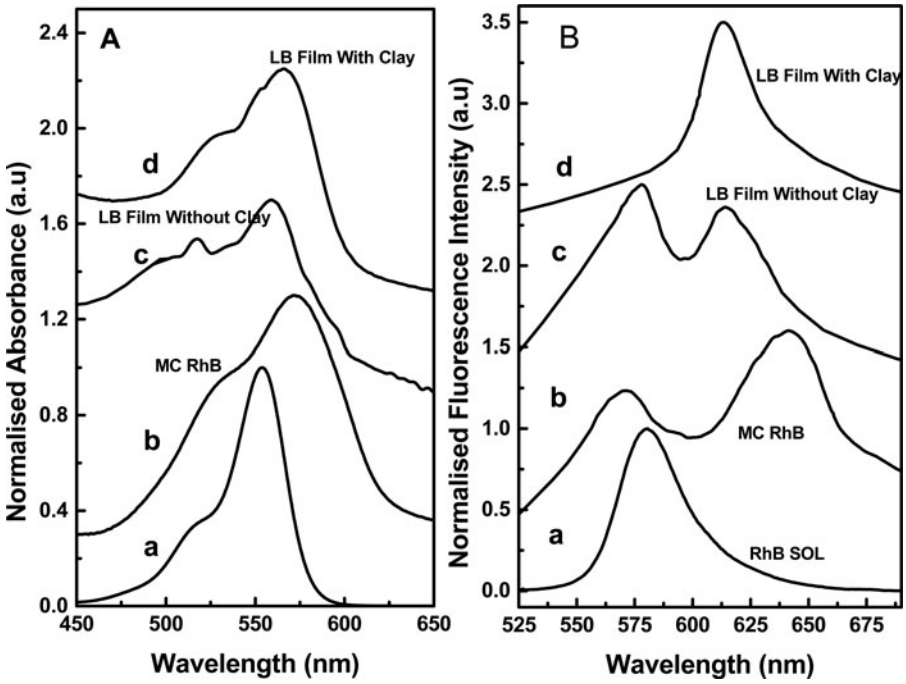

Figure 6. (A) UV-Vis absorption spectra and (B) steady state fluorescence spectra of pure RhB solution, RhB microcrystal, DPPC-RhB hybrid LB film and DPPC-RhB-clay hybrid LB film.

of clay materials only the intense longer wavelength dimeric band became prominent and shorter wavelength monomeric band was totally absent. It is due to the fact that in presence of clay platelets, RhB molecules were adsorbed on the surface of the clay platelets and came into close proximity to each other to form dimeric species.

4. Conclusions

In conclusion our results showed that the presence of nano-clay platelets highly influenced the interaction between fluorescent dye RhB and phospholipid DPPC at the air–water interface. In-situ FIM studies revealed the formation of large number of crimson red domains at the air–water interface. The domains were due to the aggregation of DPPC-RhB-Clay hybrid molecules at the air–water interface. Steady state fluorescence spectroscopic studies revealed the existence of dimeric species of RhB molecules in the LB film. This may be due to the close proximity of RhB molecules in the process of adsorption on the clay surface.

Funding

The author D. Bhattacharjee is grateful to DST for financial support through DST project Ref no: SR/S2/LOP-19/07 to carry out this research work. S. A. Hussain is grateful to DST, CSIR, and DAE for financial support through DST Fast-Track project Ref. No. SE/FTP/PS-54/2007, CSIR project Ref. 03(1146)/09/EMR-II and DAE Young Scientist Research Award (No. 2009/20/37/8/BRNS/3328).

References

[1] Monthanha, E. A., Caseli, L., Kaczmarek, O., Liebscher, J., Huster, D., *et al.* (2011). *Biophys. Chem.*, *153*, 154.
[2] Peetla, C., & Labhasetwar, V. (2008). *Mol. Pharmaceut.*, *5*, 418.
[3] Peetla, C., & Labhasetwar, V. (2009). *Langmuir*, *25*, 2369.
[4] Caro, A. L., Rodriguez Nino, M. R., & Rodriguez Patino, J. M. (2009). *Colloid Surf. A*, *341*, 134.
[5] Jablonowska, E., & Bilewicz, R. (2007). *Thin Solid Films*, *515*, 3962.
[6] Lee, K. Y. C., Gopal, A., Nahmen, A. Von, Zasadzinski, J. A., Majewski, J., *et al.* (2002). *J. Chem. Phys.*, *116*, 774.
[7] Flasinski, M., Broniatowski, M., Majewski, J., & Dynarwicz-Latka, P. (2010). *J. Colloid Interface Sci.*, *348*, 511.
[8] Bakshi, M. S., Zhao, L., Smith, R., Possmayer, F., & Petersen, N. O. (2008). *Biophys. J.*, *94*, 855.
[9] Dickinson, E. (2012). *Trends Food Sci. Technol.*, *24*, 4.
[10] Eskandar, N. G., Simovic, S., & Prestidge, C. A. (2009). *Int. J. Pharm.*, *376*, 186.
[11] Mosyanovic, A., Dausend, J., Dass, M., Walther, P., Mailander, V., *et al.* (2011). *Acta Biomater.*, *7*, 4160.
[12] Möhwald, H. (1990). *Annu. Rev. Phys. Chem.*, *41*, 441.
[13] Wüstneck, R., Perez-Gil, J., Wüstneck, N., Cruz, A., Fainerman, V. B., *et al.* (2005). *Adv. Colloid Interfaces Sci.*, *117*, 33.
[14] Zuo, Y. Y., Veldhuizen, R. A. W., Neumann, A. W., Petersen, N. O., & Possmayer, F. (2008). *Biochim. Biophys. Act.*, *1778*, 1947.
[15] Harishchandra, R. K., Saleem, M., & Galla, H.-J. (2010). *J. R. Soc. Interface*, *7*, S15.
[16] Mazzola, L. (2003). *Nat. Biotechnol.*, *21*, 1137.
[17] Hoet, P. H. M., Brüske-Hohlfeld, I., & Salata, O. V. (2004). *J. Nanobiotechnol.*, *2*, 2.
[18] Kanishtha, T., Banerjee, R., & Venkataraman, C. (2006). *Environ. Toxicol. Pharmacol.*, *22*, 325.
[19] Viseras, C., Cerezo, P., Sanchez, R., Salcedo, I., & Aguzzi, C. (2010). *Appl. Clay Sci.*, *48*, 291.
[20] Choy, J.-H., Choi, S.-J., Oh, J.-M., & Park, T. (2007). *Appl. Clay Sci.*, *36*, 122.
[21] Carretero, M. I. (2002). *Appl. Clay Sci.*, *21*, 155.
[22] Miao, S., Leeman, H., Feyter, S. D., & Schoonheydt, R. A. (2010). *J. Mater.Chem.*, *20*, 698.
[23] Lv, G., Li, Z., Jiang, W.-T., Chang, P.-H., Jean, J.-S. *et al.* (2011). *Chem. Eng. J.*, *174*, 603.
[24] Mohwald, H. (1990). *Annu. Rev. Phys. Chem.*, *41*, 441.
[25] Mohwald, H. (1993). *Rep. Prog. Phys.*, *56*, 653.
[26] Nakahara, H., Nakamura, S., Hiranita, T., Kawasaki, H., Lee, S., *et al.* (2005). *Langmuir*, *22*, 1182.
[27] Nakahara, H., Lee, S., Krafft, M. P., & Shibata, O. (2010). *Langmuir*, *26*, 18256.
[28] Mahato, M., Pal, P., Tah, B., & Talapatra, G. B. (2012). *Colloids and Surfaces A: Physicochem. Eng. Aspects*, *414*, 375.
[29] Balaswamy, B., Maganti, L., Sharma, S., & Radhakrishnan, T. P. (2012). *Langmuir*, *28*, 17313.
[30] Maherani, B., Tehrany, E. A., Kheirolomoom, A., Cleymand, F., & Linder, M. (2012). *Food Chem.*, *134*, 632.
[31] Nakahara, H., Lee, S., Shoyama, Y., & Shibata, O. (2011). *Soft Matter*, *7*, 11351.
[32] Tatur, S., & Badia, A. (2012). *Langmuir*, *28*, 628.
[33] Guzman, E., Liggieri, L., Santini, E., Ferrari, M., & Ravera, F. (2012). *Colloids and Surfaces A: Physicochem. Eng. Aspects*, *413*, 280.
[34] Guzman, E., Liggieri, L., Santini, E., Ferrari, M., & Ravera, F. (2012). *Colloids Surf. A: Physicochem. Eng. Aspects*, *413*, 174.
[35] Farnoud, A. M., & Fiegel, (2012). *J. Colloids Surf. A: Physicochem. Eng. Aspects*, *415*, 320.
[36] Preininger, C., Mohr, G. J., Klimant, I., & Wolfbeins, O. S. (1996). *Anal. Chim. Acta*, *334*, 113.
[37] Aguilera, O. V., & Neckers, D. C. (1998). *Acc. Chem. Res.*, *22*, 171.
[38] Zhang, Y. Z., X, W., & Xu, J.C. (2002). *Chin. J. Chem.*, *20*, 322.

[39] Geddes, C. D. (2002). *J. Fluoresc.*, *12*, 343.
[40] Biswas, S., Hussain, S. A., Deb, S., Nath, R. K., & Bhattacherjee, D. (2006). *Spectrochim. Acta Part A*, *65*, 628.
[41] Biswas, S., Bhattacherjee, D., Nath, R. K., & Hussain, S. A. (2007). *J. Colloid Interface Sci.*, *311*, 361.
[42] Cristoflini, L., Berzina, T., Erokhina, S., Konovalov, O., & Erokhin, V. (2007). *Biomacromolecules*, *8*, 2270.
[43] Slote, J. P., & Mattjus, P. (1995). *Biochimica et Biophysica. Acta*, *1254*, 22.
[44] Muto, J. (1972). *Jpn. J. Appl. Phys.*, *11*, 1217.
[45] Kemnitz, K., Tamai, N., Yamazaki, I., Nakashima, N., & Yoshihara, K. (1986). *J. Phys. Chem.*, *90*, 5094.